miR-106b-5p targeting SIX1 inhibits TGF-β1-induced pulmonary fibrosis and epithelial-mesenchymal transition in asthma through regulation of E2F1

SHUANG LIU[1*], XI CHEN[1*], SIQING ZHANG[2*], XINYU WANG[1], XIAOLIU DU[3], JIAHE CHEN[1] and GUOPING ZHOU[1]

[1]Department of Pediatrics, The First Affiliated Hospital of Nanjing Medical University; [2]Department of Respiratory Medicine, Children's Hospital of Nanjing Medical University; [3]Department of Pathology, The First Affiliated Hospital of Nanjing Medical University, Nanjing, Jiangsu 210029, P.R. China

Received July 11, 2020; Accepted December 21, 2020

DOI: 10.3892/ijmm.2021.4857

Abstract. Asthma is an inflammatory disease of the airways, characterized by lung eosinophilia, mucus hypersecretion by goblet cells and airway hyper-responsiveness to inhaled allergens. The present study aimed to identify the function of microRNA (miR/miRNA)-106b-5p in TGF-β1-induced pulmonary fibrosis and epithelial-mesenchymal transition (EMT) via targeting sine oculis homeobox homolog 1 (SIX1) through regulation of E2F transcription factor 1 (E2F1) in asthma. Asthmatic mouse models were induced with ovalbumin. miRNA expression was evaluated using reverse transcription-quantitative PCR. Transfection experiments using bronchial epithelial cells were performed to determine the target genes. A luciferase reporter assay system was applied to identify the target gene of miR-106b-5p. The present study revealed downregulated miR-106b-5p expression and upregulated SIX1 expression in asthmatic mice and TGF-β1-induced BEAS-2B cells. Moreover, miR-106b-5p overexpression inhibited TGF-β1-induced fibrosis and EMT in BEAS-2B cells, while miR-106b-5p-knockdown produced the opposite effects. Subsequently, miR-106b-5p was found to regulate SIX1 through indirect regulation of E2F1. Additionally, E2F1- and SIX1-knockdown blocked TGF-β1-induced fibrosis and EMT in BEAS-2B cells. In addition, miR-106b-5p negatively regulated SIX1 via E2F1 in BEAS-2B cells. The present study demonstrated that the miR-106b-5p/E2F1/SIX1 signaling pathway may provide potential therapeutic targets for asthma.

Correspondence to: Professor Guoping Zhou, Department of Pediatrics, The First Affiliated Hospital of Nanjing Medical University, 300 Guang Zhou Road, Nanjing, Jiangsu 210029, P.R. China
E-mail: gpzhou2017@126.com

*Contributed equally

Key words: asthma, epithelial-mesenchymal transition, microRNA-106b-5p, E2F transcription factor 1, sine oculis homeobox homolog 1

Introduction

Asthma is a severe chronic inflammatory disease with an increasing prevalence worldwide (1,2). The pathogenesis of asthma involves complicated factors, including immunity, infection, environmental factors and genetic inheritance (3). Airway remodeling, a typical characteristic of asthma, is manifested by airway wall thickening, subepithelial fibrosis, increased smooth muscle mass, angiogenesis and increased mucous glands (4,5).

MicroRNAs (miRNAs/miRs) are non-coding RNAs of 20-25 nucleotides that cannot be further translated into proteins, but can suppress gene expression by binding to the 3'-untranslated region (3'-UTR) of target mRNAs (6,7). Accumulating research has shown that miRNAs participate in numerous biological processes, such as cell proliferation (8), differentiation (9), apoptosis (10) and epithelial-mesenchymal transition (EMT) (11). Additionally, a previous study has revealed the important role of miRNAs in mouse models of asthma (12). miR-106b-5p has been associated with glioma tumorigenesis (13), lung cancer (14), chronic myeloid leukemia (15), breast cancer (16,17) and hepatocellular carcinoma (18). However, the molecular mechanisms of miR-106b-5p in asthma remain unclear.

The purpose of the present study was to investigate the function of miR-106b-5p in TGF-β1-induced pulmonary fibrosis and EMT, the therapeutic effect of miR-106b-5p in asthma and the underlying mechanisms.

Materials and methods

Cell culture and chemicals. Human bronchial epithelial cells (BEAS-2B) were purchased from the American Type Culture Collection and were cultivated in DMEM supplemented with 10% FBS (both Gibco; Thermo Fisher Scientific, Inc.), penicillin (100 U/ml) and streptomycin (100 mg/ml) in a humidified incubator containing 5% CO_2 at 37˚C. BEAS-2B

cells were treated with TGF-β1 (Abcam; 10 ng/ml) at 37˚C for 24 h.

Ovalbumin (OVA)-induced murine asthma model. A total of 10 BALB/c male mice (6 weeks old; 18-20 g), obtained from Beijing Vital River Laboratory Animal Technology Co. Ltd. Mice were housed in plastic boxes with a 12-h light/dark cycle and constant temperature (19-23˚C) and humidity (55±10%). Food and water were supplied *ad libitum*. Mice were randomized into two groups: The control group and the OVA group, each group containing 5 mice. On day 0 and day 14, the mice of the OVA group were sensitized with 20 μg OVA (Sigma-Aldrich; Merck KGaA) with 1 mg aluminum hydroxide (Thermo Fisher Scientific, Inc.) adsorbed in 200 μl PBS by intraperitoneal injection. On days 21-23, the mice of the OVA group were challenged through the airway with 1% OVA (dissolved in PBS) for 30 min using an ultrasonic nebulizer (INQUA NEB Plus; PARI GmbH). The mice of the control group were treated with PBS. All the mice were euthanized by cervical dislocation on day 24. The present study was approved by the Nanjing Medical University Animal Experimental Ethics Committee (approval no. 2005020).

Plasmids, small interfering RNAs (siRNAs) and miRNA mimic or antimiR. The transcriptional start site of human sine oculis homeobox homolog 1 (SIX1) promoter was set as +1. The promoter of SIX1 DNA fragment -351 to +100 was inserted into the pGL3-Basic vector (Promega Corporation) and named pGL3-451. The transcriptional binding sites of SIX1 were predicted using the JASPAR database (version 5.0; jaspar.genereg.net) (19). A series of plasmids with mutations of E2F transcription factor 1 (E2F1)-binding sites were synthesized from TsingKe Biological Technology. According to the binding sites, a series of pGL3-mut plasmids were generated, named mut-E2F1-A, mut-E2F1-B and mut-E2F1-A+B. The mutated sequence of the E2F1-A binding site (-64 ATAGGC GCCGCC-53) was 5'-ATATTATAAGCC-3', and the mutated sequence of the E2F1-B binding site (+41 CGGGCGGGA GG +51) was 5'-CGGATAGGTGG-3'. The overexpression plasmid pENTER-E2F1 (pE2F1) and the corresponding control plasmid pENTER (TsingKe Biological Technology) were supplied by our lab (20). The double-stranded siRNAs (Table I) were synthesized and purified by high-performance chromatography by Shanghai GenePharma Co., Ltd. The sequences of the miR mimics and antimiR (both Guangzhou RiboBio Co., Ltd.) are listed in Table I. The type of negative controls used was non-targeting.

Transient transfections and luciferase assays. Transfections were conducted in BEAS-2B cells using Lipofectamine® 3000 (Invitrogen; Thermo Fisher Scientific, Inc.). A total of 100 nM antimiR-106b-5p and 50 nM miR-106b-5p mimics was used for transfection at 37˚C for 48 h, after which cells were harvested for subsequent experimentation. Cells were seeded into 96-well plates ($1x10^4$ cells/well). A total of 100 ng of the promoter reporter plasmids (pGL3-451 and pGL3-mut) together with the pRL-TK plasmid (used as an internal control reporter vector; 4 ng; Promega Corporation) were co-transfected into cells as an internal control using Lipofectamine 3000 at 37˚C for 48 h according to the manufacturer's protocol. For siRNA and overexpression assays, pGL3-451 or pGL3-mut plasmids were co-transfected with siE2F1 (50 nM) or pENTER-E2F1 (100 ng) into cells. After 24 h from transfection, promoter activity was assessed using a Dual-Luciferase Reporter Assay System (Promega Corporation) and normalized to the activity of pRL-TK (*Renilla* luciferase activity). The E2F1 wild-type (WT) 3'-UTR was cloned into the pmiR-RB-reporter (TsingKe Biological Technology) and the mutated putative miR-106b-5p binding site in the E2F1 3'-UTR was cloned into the pmiR-RB-reporter and named E2F1 mutant (MUT) 3'-UTR. The SIX1 WT 3'-UTR was cloned into the pmiR-RB-reporter and named pmiR-RB-SIX1 plasmid (TsingKe Biological Technology) and cells were co-transfected using three different concentrations (50, 100 and 150 nM) of miR-106b-5p mimic. The results were representative of at least three independent experiments conducted in triplicate.

Reverse transcription-quantitative (RT-qPCR). Total RNA was extracted from mouse tissues and cell lines using TRIzol® reagent (Invitrogen; Thermo Fisher Scientific, Inc.), and then reverse-transcribed into first strand cDNA using the PrimeScript RT Master Mix Perfect Real Time kit (Takara Biotechnology Co., Ltd.) according to the manufacturer's protocol. qPCR was conducted in a LightCycler480II (Roche Diagnostics) with TB Green technology (Takara Biotechnology Co., Ltd.). The thermocycling conditions were as follows: Initial denaturation for 30 sec at 95˚C, followed by 40 cycles of denaturation for 5 sec at 95˚C, annealing for 30 sec at 55˚C and extension for 30 sec at 72˚C. The total mRNA levels were analyzed in triplicate with β-actin as a normalized standard, while miR expression was normalized to U6. The relative expression levels were evaluated using the $2^{-\Delta\Delta Cq}$ method (21). The specific primers (Guangzhou RiboBio Co., Ltd.) are listed in Table II.

Hematoxylin and eosin (H&E) staining and immunohistochemistry (IHC). Tissues for H&E and IHC were collected from asthmatic mice model and control mice. The lungs of mice were harvested and fixed in 4% paraformaldehyde for 24 h at room temperature and then embedded in paraffin using a standard protocol after dehydration. Subsequently, 4-μm-thick sections of embedded lung tissue were mounted onto slides and stained with H&E for 5 min at room temperature to identify tissue inflammation. Tissue sections were viewed with a light microscope (magnification, x100). The expression levels of E2F1 and SIX1 were evaluated by semi-quantitative IHC according to a previous study (22). After paraffin removal, sections were incubated in 0.01 mol/l citric acid buffer (pH 6.0) in a microwave for 15 min at 95˚C for antigen recovery. Subsequently, sections were washed with xylene and rehydrated in a descending alcohol series. The sections were then cooled and incubated in 3 g/l H_2O_2 for 30 min at room temperature to inactivate endogenous peroxidase, then blocked with 1:10 normal goat serum (Gibco; Thermo Fisher Scientific, Inc.) at room temperature for 30 min. Subsequently, the supernatant was discarded and primary anti-mouse E2F1 (1:400; cat. no. ab179445; Abcam) and SIX1 (1:500; cat. no. 10709-1-AP; ProteinTech Group, Inc.) antibodies were added overnight at 4˚C, followed by biotinylated goat anti-rabbit secondary antibody (1:500;

Table I. Sequences used for siRNAs, miR mimic and antimiR.

Name	Sequence (5'-3')
siE2F1	Sense: CACUGAAUCUGACCACCAATT
	Antisense: UUGGUGGUCAGAUUCAGUGTT
siSIX1	Sense: GCAUCAGCUCCAAGACUCUTT
	Antisense: AGAGUCUUGGAGCUGAUGCTT
siNC	Sense: UUCUCCGAACGUGUCACGUTT
	Antisense: ACGUGACACGUUCGGAGAATT
miR-106b-5p mimic	Sense: UAAAGUGCUGACAGUGCAGAU
	Antisense: AUCUGCACUGUCAGCACUUUA
mimic NC	Sense: UUUGUACUACACAAAAGUACUG
	Antisense: CAGUACUUUUGUGUAGUACAAA
antimiR-106b-5p	AUCUGCACUGUCAGCACUUUA
antimiR-NC	CAGUACUUUUGUGUAGUACAAA

siRNA, small interfering RNA; miR, microRNA; NC, negative control; E2F1, E2F transcription factor 1; SIX1, sine oculis homeobox homolog 1.

Table II. Primers used for reverse transcription-quantitative PCR.

Gene	Forward primer (5'-3')	Reverse-primer (5'-3')
E2F1	AGCGGCGCATCTATGACATC	GTCAACCCCTCAAGCCGTC
SIX1	AAGGAGAAGTCGAGGGGTGT	TGCTTGTTGGAGGAGGAGTT
β-actin	AAAGACCTGTACGCCAACAC	GTCATACTCCTGCTTGCTGAT
E-cadherin	CGAGAGCTACACGTTCACGG	GGGTGTCGAGGGAAAAATAGG
N-cadherin	TCAGGCGTCTGTAGAGGCTT	ATGCACATCCTTCGATAAGACTG
Vimentin	GACGCCATCAACACCGAGTT	CTTTGTCGTTGGTTAGCTGGT
Fibronectin	CGGTGGCTGTCAGTCAAAG	AAACCTCGGCTTCCTCCATAA
Collagen IV	GGACTACCTGGAACAAAAGGG	GCCAAGTATCTCACCTGGATCA
α-SMA	AAGAGGAAGACAGCACAGCTC	GATGGATGGGAAAACAGCC
miR-106b-5p	CTGGAGTAAAGTGCTGACAGTG	GTGCAGGGTCCGAGGT
U6	GCTTCGGCAGCACATATACTAAAAT	CGCTTCACGAATTTGCGTGTCAT

E2F1, E2F transcription factor 1; SIX1, sine oculis homeobox homolog 1; SMA, smooth muscle actin; miR, microRNA.

cat. no. SA00001-2; ProteinTech Group, Inc.) for 30 min at room temperature and streptavidin-horseradish peroxidase (1:500; cat. no. A0303; Beyotime Institute of Biotechnology) for 30 min at room temperature. The stained cells were then immobilized and observed under a light microscope (magnification, x200).

Western blotting. Cell lysis buffer (Beyotime Institute of Biotechnology) containing 0.1 mM phenylmethylsulfonyl fluoride (a protease inhibitor) and phosphatase inhibitors (Nanjing KeyGen Biotech Co., Ltd.), was used to lyse the cells and tissues. Protein concentrations were measured using a bicinchoninic acid assay. Protein samples (30-50 μg/lane) were separated via 8 and 12% SDS-PAGE and transferred to PVDF membranes, which were subsequently incubated with 5% dry milk in TBS-T saline [0.25 M Tris-HCl (pH 7.6), 0.19 M NaCl and 0.1% Tween 20] for 2 h at room temperature to block non-specific binding. The protein blots were incubated overnight at 4˚C with primary antibodies against GAPDH (1:4,000; ProteinTech Group, Inc.; cat. no. 60004-1-Ig), E2F1 (1:1,000; Abcam; cat. no. ab179445), SIX1 (1:1,000; ProteinTech Group, Inc.; cat. no. 10709-1-AP), collagen IV (1:2,000; Abcam; cat. no. ab182744), fibronectin (1:1,000; ProteinTech Group, Inc.; cat. no. 15613-1-AP), α-smooth muscle actin (SMA; 1:2,000; Abcam; cat. no. ab7817), E-cadherin (1:4,000; Abcam; cat. no. ab40772), N-cadherin (1:4,000; Abcam; cat. no. ab76011) and vimentin (1:1,000; Abcam; cat. no. ab92547) diluted with primary antibody dilution buffer (Beyotime Institute of Biotechnology). Subsequently, the membranes were washed thrice with TBS-T and treated with HRP-conjugated goat anti-rabbit IgG (1:3,000; ProteinTech Group, Inc.; cat. no. SA00001-2) or anti-mouse IgG (1:3,000; ProteinTech Group, Inc.; cat. no. SA00001-1) diluted with secondary antibody dilution buffer (Beyotime Institute of

Biotechnology) at room temperature for 2 h. The blots were then developed by incubation in a chemiluminescence substrate (SuperSignal West Femto Maximum Sensitivity Substrate; Thermo Fisher Scientific, Inc.) and exposed to X-ray films.

Chromatin immunoprecipitation (ChIP) assay. The ChIP assay was performed using the EZ-Magna Chip A kit (EMD Millipore; cat. no. 17-10086) following the manufacturer's instructions. A total of $1x10^7$ BEAS-2B cells were fixed with 1% formaldehyde for 10 min at room temperature, and stopped by addition of glycine to a final concentration of 0.125 M. Fixed cells were harvested in 2 ml PBS buffer with protease inhibitors. Cells were pelleted using centrifugation (800 x g at 4˚C for 5 min) and suspended in 0.5 ml nuclear lysis buffer. Cells were sonicated with a 0.25-inch diameter probe for 7W, 15 sec twice at 4˚C and span at 10,000 x g at 4˚C for 10 min to remove insoluble material. For each immunoprecipitation, 450 μl lysates was used. Samples were spun, and the supernatants were incubated at 4˚C for 3 h with either no antibody, anti-IgG control antibody (1.0 μg; EMD Millipore) or anti-E2F1 antibody (10.0 μg; Abcam; cat. no. ab179445) to be tested. Immune complexes were recovered by adding 20 μl blocked protein A/G beads and incubated at 4˚C overnight. Pellet protein A/G magnetic beads were isolated using a magnetic separator. DNA fragment extraction from beads was performed using the ChIP assay kit. For ChIP-qPCR analysis, the purified DNA from input or immunoprecipitated samples were assayed by qPCR with SYBR Green I Master Mix (Takara Bio, Inc.) after reverse cross-linking and DNA purification. The primers used were as follows: Forward, 5'-CTT CCTTCTCCTCCCACCACTCC-3' and reverse, 5'-CCGGCG CACTCAGTAGCCTTT-3'.

Statistical analysis. Statistical analyses were conducted using SPSS 22.0 (IBM Corp.). All data were presented as the mean ± SD from three independent experiments. The differences among multiple groups were analyzed using one-way ANOVA with repeated measures followed by Tukey's post-hoc test, while differences between two groups by Student's unpaired t-test. The correlation between various factors was analyzed using Pearson's correlation analysis. TargetScanHuman v7.2 (http://www.targetscan.org/vert_72/) and StarBase v2.0 (http://starbase.sysu.edu.cn/starbase2/) were used to predict miRNA-targeting genes. $P<0.05$ was considered to indicate a statistically significant difference.

Results

miR-106b-5p expression is downregulated and SIX1 expression is upregulated in mice with asthma and TGF-β1-induced BEAS-2B cells. To investigate whether miR-106b-5p expression was different *in vivo*, a mouse model of asthma was established in the present study. Fig. 1A shows the treatment schedule of asthmatic mice model and the control group. The difference was further verified by hematoxylin and eosin staining of lung sections (Fig. 1B). The control group exhibited a very small amount of inflammatory cell infiltration, without thickening of bronchial wall (Fig. 1Ba). A moderate number of neutrophils and a small amount of eosinophil infiltration was observed at the bronchial wall and surrounding tissue of the OVA group, with slightly thickened wall (Fig. 1Bb). RT-qPCR was performed to estimate miR-106b-5p expression in the mouse model with airway remodeling induced by repetitive OVA challenge and in control mice. miR-106b-5p expression was significantly decreased in asthmatic mice compared with in control mice (Fig. 1C). Yang *et al* (23) demonstrated that SIX1 downregulation effectively suppressed airway inflammation and reversed airway remodeling in mice with asthma. Hence, the present study investigated whether there was an association between miR-106b-5p and SIX1. Therefore, mRNA and protein expression levels of SIX1 were also analyzed (Fig. 1D and F), and the correlation between miR-106b-5p and SIX1 expression was determined (Fig. 1E). SIX1 expression was significantly increased in the asthma group compared with in the control group and was negatively correlated with miR-106-5p expression. Furthermore, SIX1 expression in the mouse lung tissues was evaluated using IHC, revealing that SIX1 staining displayed higher intensity in lung tissues from the asthmatic mice group compared with those from the control mice (Fig. 1G). Additionally, SIX1 expression in the IHC analysis was quantified, revealing that SIX1 expression was significantly increased in the asthma group compared with in the control group (Fig. 1K). *In vitro*, miR-106b-5p expression was analyzed in BEAS-2B cells after treatment with TGF-β1 (10 ng/ml) for 6, 12, 24 and 48 h, revealing that miR-106b-5p expression was significantly decreased in TGF-β1-induced BEAS-2B cells compared with the control group at 24 and 48 h (Fig. 1H). SIX1 expression was significantly increased in BEAS-2B cells treated with TGF-β1 (10 ng/ml) for 24 h (Fig. 1I and J).

miR-106b-5p inhibits TGF-β1-induced fibrosis and EMT in BEAS-2B cells. To further explore the function of miR-106b-5p in TGF-β1-stimulated fibrosis and EMT in BEAS-2B cells, miR-106b-5p mimics or antimiR-106b-5p were transfected into TGF-β1-stimulated BEAS-2B cells. Firstly, RT-qPCR was employed to detect miR-106b-5p expression after transfection. In BEAS-2B cells, a 12.04-fold increase or a 4.13-fold decrease was detected in miR-106b-5p mRNA expression after transfection with the miR-106b-5p mimic or antimiR-106b-5p, respectively (Fig. 2A and B), indicating a high efficiency of transfection for subsequent experiments. Secondly, the mRNA expression levels of α-SMA, fibronectin and collagen IV were assessed to define the function of miR-106b-5p in TGF-β1-stimulated fibrosis in BEAS-2B cells. TGF-β1 treatment increased the expression levels of α-SMA, fibronectin and collagen IV in BEAS-2B cells. The data suggested that compared with TGF-β1 treatment alone, the overexpression of miR-106b-5p suppressed α-SMA, fibronectin and collagen IV in TGF-β1-induced BEAS-2B cells, while miR-106b-5p-knockdown aggravated TGF-β1-stimulated fibrosis (Fig. 2C and D). In addition, the results indicated that the overexpression or knockdown of miR-106b-5p did not exert effects on fibrosis without TGF-β1 treatment (Fig. 2C and D). Thirdly, the mRNA expression levels of EMT-associated markers, including E-cadherin, N-cadherin and vimentin, were detected by RT-qPCR to identify whether miR-106b-5p affected EMT in TGF-β1-stimulated BEAS-2B cells. TGF-β1 treatment increased the expression levels of the mesenchymal markers (N-cadherin and vimentin) and decreased the expression levels of the epithelial marker E-cadherin in BEAS-2B

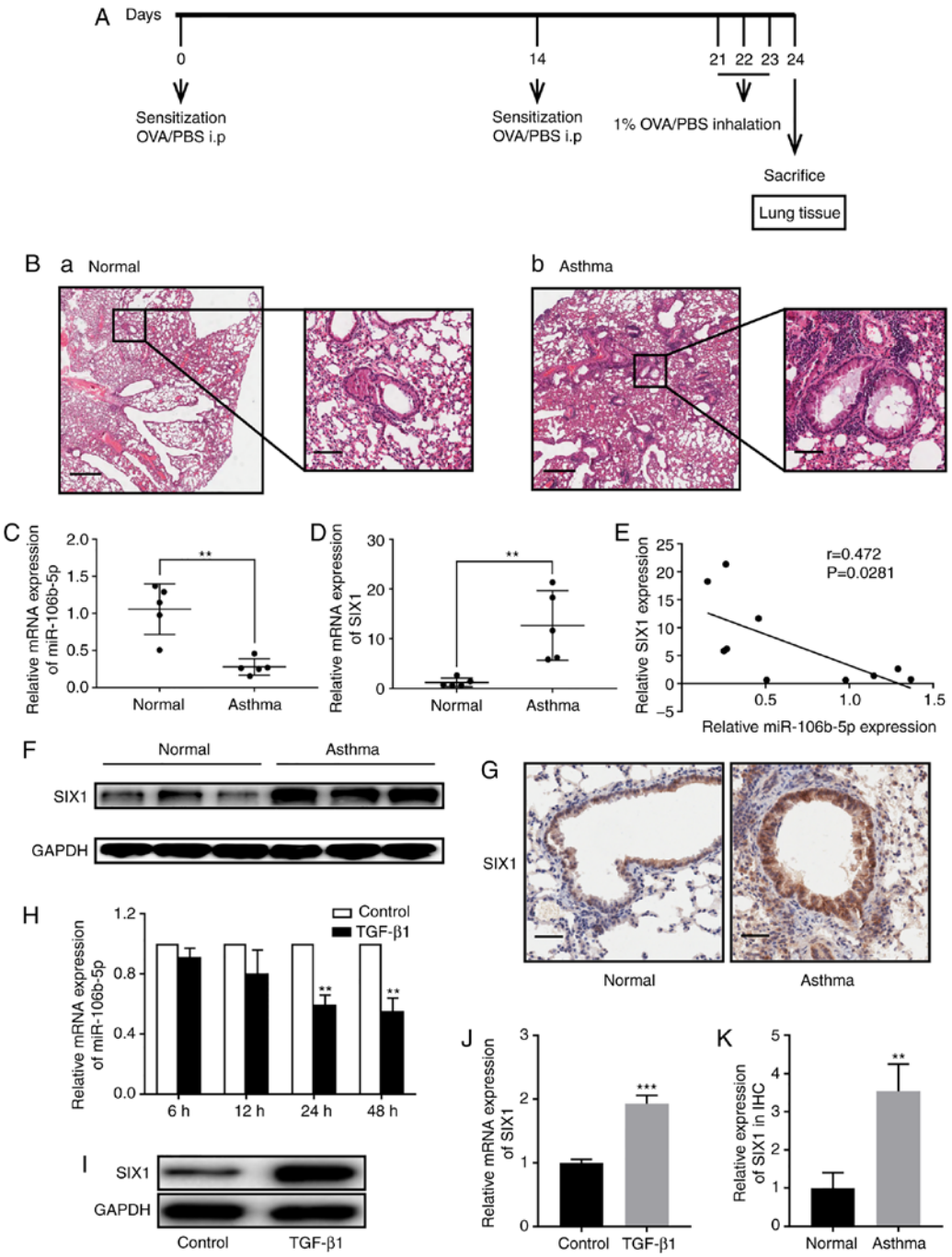

Figure 1. miR-106b-5p and SIX1 expression in asthmatic mice and TGF-β1-induced BEAS-2B cells. (A) Treatment schedule of asthmatic mice model and control group. (B) Lung tissues in (a) normal and (b) asthmatic mice model (scale bar, 500 and 100 μm). Relative expression levels of (C) miR-106b-5p and (D) SIX1 in asthmatic (n=5) and normal mice (n=5) were measured by RT-qPCR. (E) Pearson's correlation analysis between miR-106b-5p and SIX1 expression. (F) SIX1 protein expression in asthmatic and normal mice. (G) SIX1 expression in the lung tissues of asthmatic and normal mice was evaluated via IHC (scale bar, 50 μm). (H) After TGF-β1 (10 ng/ml) treatment for 6, 12, 24 and 48 h, miR-106b-5p expression in BEAS-2B cells was analyzed by RT-qPCR. (I) Western blotting and (J) RT-qPCR were performed to detect the protein and mRNA expression levels of SIX1, respectively, in BEAS-2B cells after treatment with or without TGF-β1 (10 ng/ml) for 24 h. (K) Quantification of SIX1 expression according to IHC. Data are presented as the mean ± SD of three independent experiments. **P<0.01; ***P<0.001. miR, microRNA; SIX1, SIX1, sine oculis homeobox homolog 1; RT-qPCR, reverse transcription-quantitative PCR; IHC, immunohistochemistry.

cells (Fig. 2E and F). The data suggested that compared with TGF-β1 treatment alone, miR-106b-5p overexpression in TGF-β1-induced cells negatively regulated the expression levels of the mesenchymal markers (N-cadherin and vimentin) and positively regulated the expression levels of the epithelial marker E-cadherin, while miR-106b-5p-knockdown aggravated TGF-β1-stimulated EMT (Fig. 2E and F). Additionally, the overexpression or inhibition of miR-106b-5p alone did not affect the basal gene expression levels in BEAS-2B cells (Fig. 2E and F).

miR-106b-5p does not bind to the consensus sequences in the 3'-UTR of SIX1 mRNA. To explore the association between miR-106b-5p and SIX1, western blotting and

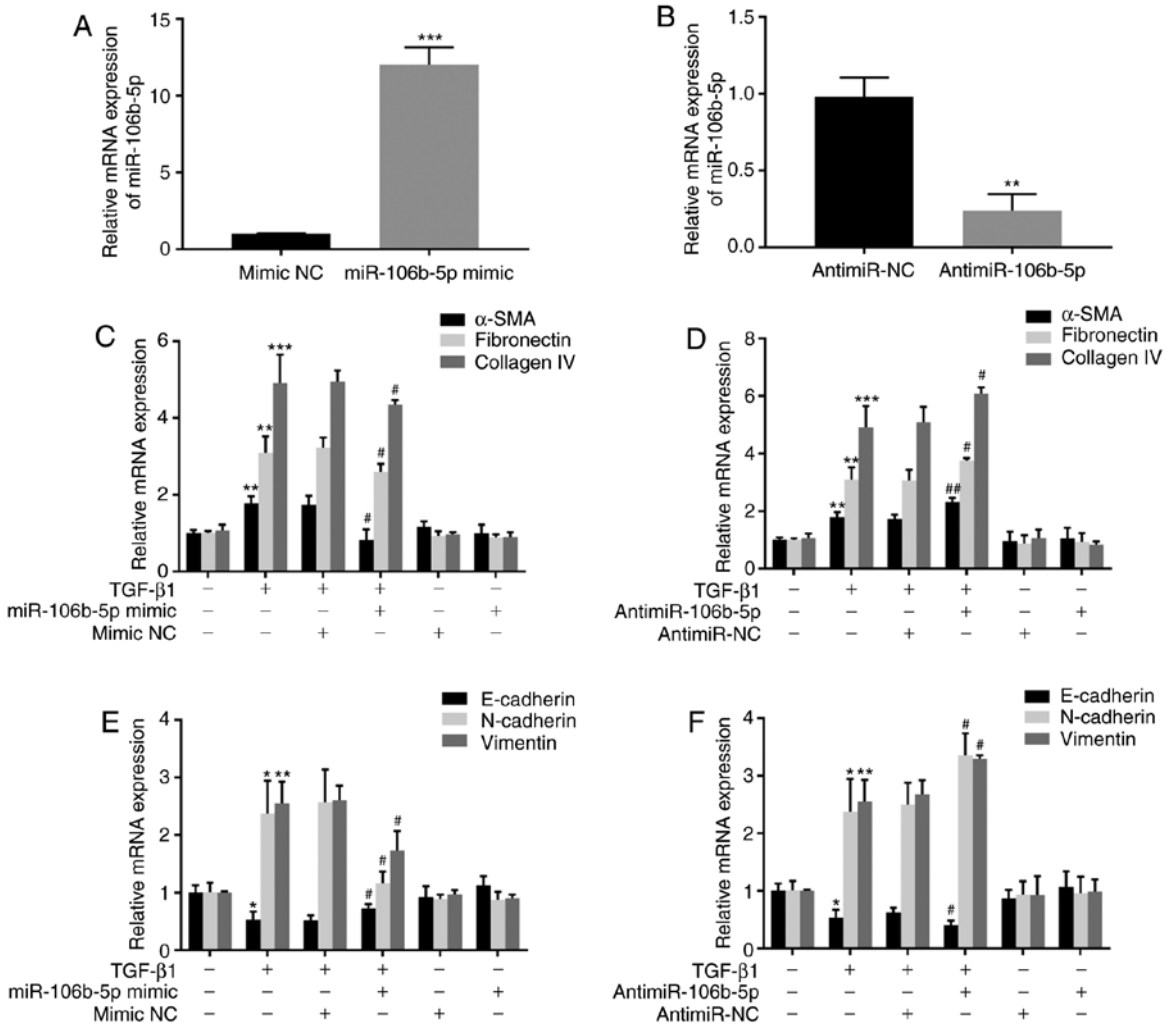

Figure 2. Effect of miR-106b-5p on TGF-β1-induced fibrosis and EMT in BEAS-2B cells. miR-106b-5p expression in BEAS-2B cells following (A) miR-106b-5p mimic or (B) antimiR-106b-5p transfection was determined by RT-qPCR. RT-qPCR was performed to detect the mRNA expression levels of fibrosis-associated proteins α-SMA, fibronectin and collagen IV in (C) miR-106b-5p-mimic- or (D) antimiR-106b-5p-transfected BEAS-2B cells after treatment with or without TGF-β1 for 24 h. RT-qPCR was conducted to detect the mRNA expression levels of EMT-associated proteins E-cadherin, N-cadherin and vimentin in (E) miR-106b-5p-mimic- or (F) antimiR-106b-5p-transfected BEAS-2B cells after treatment with or without TGF-β1 for 24 h. Data are presented as the mean ± SD of three independent experiments. *P<0.05, **P<0.01 and ***P<0.001 vs. control. $^{\#}$P<0.05 and $^{\#\#}$P<0.01 vs. mimic-NC+TGF-β1 or antimir-NC+TGF-β1. miR, microRNA; RT-qPCR, reverse transcription-quantitative PCR; NC, negative control; SMA, smooth muscle actin; EMT, epithelial-mesenchymal transition.

RT-qPCR were employed to measure SIX1 expression in miR-106b-5p-mimic-transfected or antimiR-106b-5p-transfected BEAS-2B cells. SIX1 expression was significantly decreased after miR-106b-5p mimic transfection and significantly increased after antimiR-106b-5p transfection, compared with their respective negative controls (Fig. 3A and B). miRNAs function by downregulating downstream genes by guiding the cytoplasmic RNA-induced silencing complexes targeting the 3'-UTR of mRNAs to suppress their translation or induce their degradation (6). Thus, the present study explored the potential effects of miR-106b-5p on the inhibition of mRNA function by binding to consensus sequences in the 3'-UTR of SIX1. However, the effects of miR-106b-5p on SIX1 mRNA targets could not be determined using TargetScanHuman v7.2. To further investigate the influence of miR-106b-5p on SIX1, the pmiR-RB-SIX1 reporter plasmid and three different concentrations of miR-106b-5p mimic were transfected into BEAS-2B cells. Subsequently, the dual-luciferase assay detection kit revealed that miR-106b-5p did not have a regulatory effect on the SIX1 3'-UTR (Fig. 3C and D).

miR-106b-5p directly targets E2F1. E2F1 was identified as a target gene of miR-106b-5p using TargetScan and StarBase v2.0. Hence, the mRNA and protein expression levels of E2F1 were analyzed in asthmatic and control mice, revealing that E2F1 expression was significantly increased in the asthma group compared with in the control group (Fig. 4A and B). Additionally, E2F1 expression in the mouse lung tissues was evaluated using IHC, revealing that E2F1 staining displayed a higher intensity in lung tissues from the asthmatic mice group compared with those from the control group (Fig. 4C). E2F1 expression in the IHC analysis was also quantified, revealing that E2F1 expression was significantly increased in the asthma group compared with in the control group (Fig. 4D). Furthermore, E2F1 expression was significantly increased in BEAS-2B cells treated with 10 ng/ml for 24 h (Fig. 4F). To investigate the association between miR-106b-5p and E2F1, the E2F1 WT and MUT

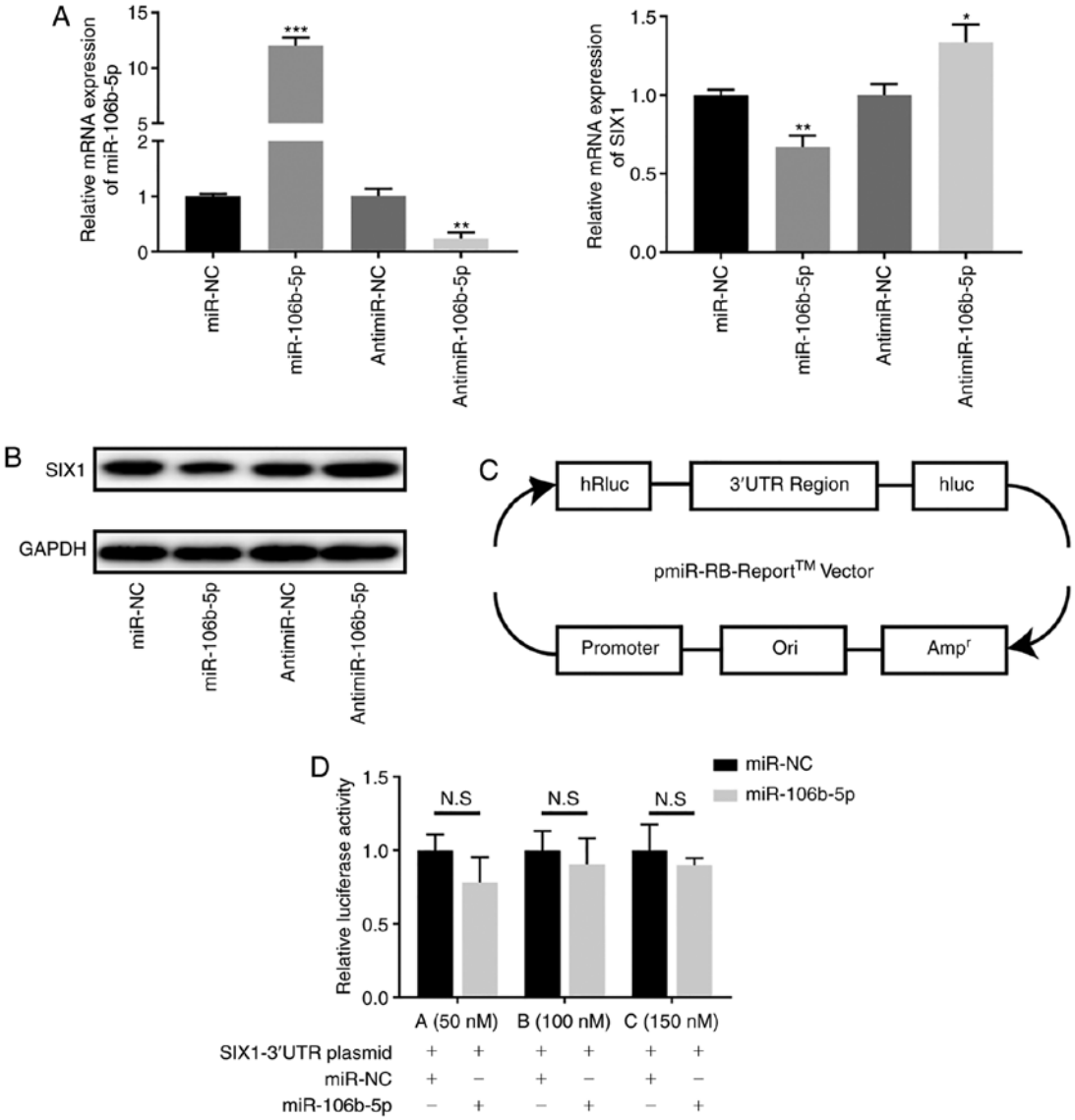

Figure 3. Association between miR-106b-5p and SIX1. (A) miR-106b-5p and SIX1 mRNA expression in miR-106b-5p-mimic- (50 nM) or antimiR-106b-5p-transfected (100 nM) BEAS-2B cells. (B) Western blotting was performed to detect the protein expression levels of SIX1 after transfecting BEAS-2B cells with miR-106b-5p-mimic or antimiR-106b-5p. (C) Structure of SIX1-3'-UTR plasmid, pmiR-RB-reporter construct in TM-SIX1 mRNA 3'-UTR of a reporter plasmid containing the SV40 promoter-driven fluorescence reporter, downstream of the SIX1 mRNA 3'-UTR construct. (D) Luciferase reporter plasmids containing the wild-type SIX1-3'UTR were co-transfected into BEAS-2B cells with miR-106b-5p (50, 100 or 150 nM) to detect the luciferase activity. Data are presented as the mean ± SD of three independent experiments. *P<0.05, **P<0.01 and ***P<0.001 vs. respective NCs. NS, not significant; miR, microRNA; SIX1, SIX1, sine oculis homeobox homolog 1; NC, negative control; UTR, untranslated region.

3'-UTRs were cloned into the pmiR-RB-reporter (Fig. 4E). The results demonstrated that the miR-106b-5p mimic significantly suppressed luciferase activity in BEAS-2B cells treated with the E2F1 WT 3'-UTR, but did not have influence on BEAS-2B cells treated with the E2F1 MUT 3'-UTR (Fig. 4E). Subsequently, western blotting and RT-qPCR were employed to measure E2F1 expression in miR-106b-5p-mimic- or antimiR-106b-5p-transfected BEAS-2B cells, revealing that E2F1 expression was significantly decreased after miR-106b-5p mimic transfection and significantly increased after antimiR-106b-5p transfection (Fig. 4G and H), compared with their respective negative controls.

E2F1 regulates SIX1 at the transcriptional level. To explore whether E2F1 could regulate SIX1 transcription directly, a sequence from -351 to +100 upstream of the human SIX1 promoter was cloned into pGL3-451. By scanning this promoter region using the JASPAR database, two potential binding sites and the key nucleotides of E2F1 were found (Fig. 5A). After co-transfecting pGL3-451 with plasmids containing siE2F1 or pE2F1, the luciferase activity of SIX1 was significantly increased by E2F1 overexpression and significantly decreased by siE2F1 (Fig. 5B). Subsequently, a series of plasmids with point mutations of E2F1 binding sites were cloned and were then transfected into BEAS-2B cells. As demonstrated by Fig. 5C, E2F1-A and E2F1-B mutations in BEAS-2B cells significantly inhibited the promoter activity, as well as E2F1-A+B mutations. Additionally, when siE2F1 or pE2F1 were co-transfected with the mutations of E2F1-A+B into BEAS-2B cells, there were no significant changes in luciferase

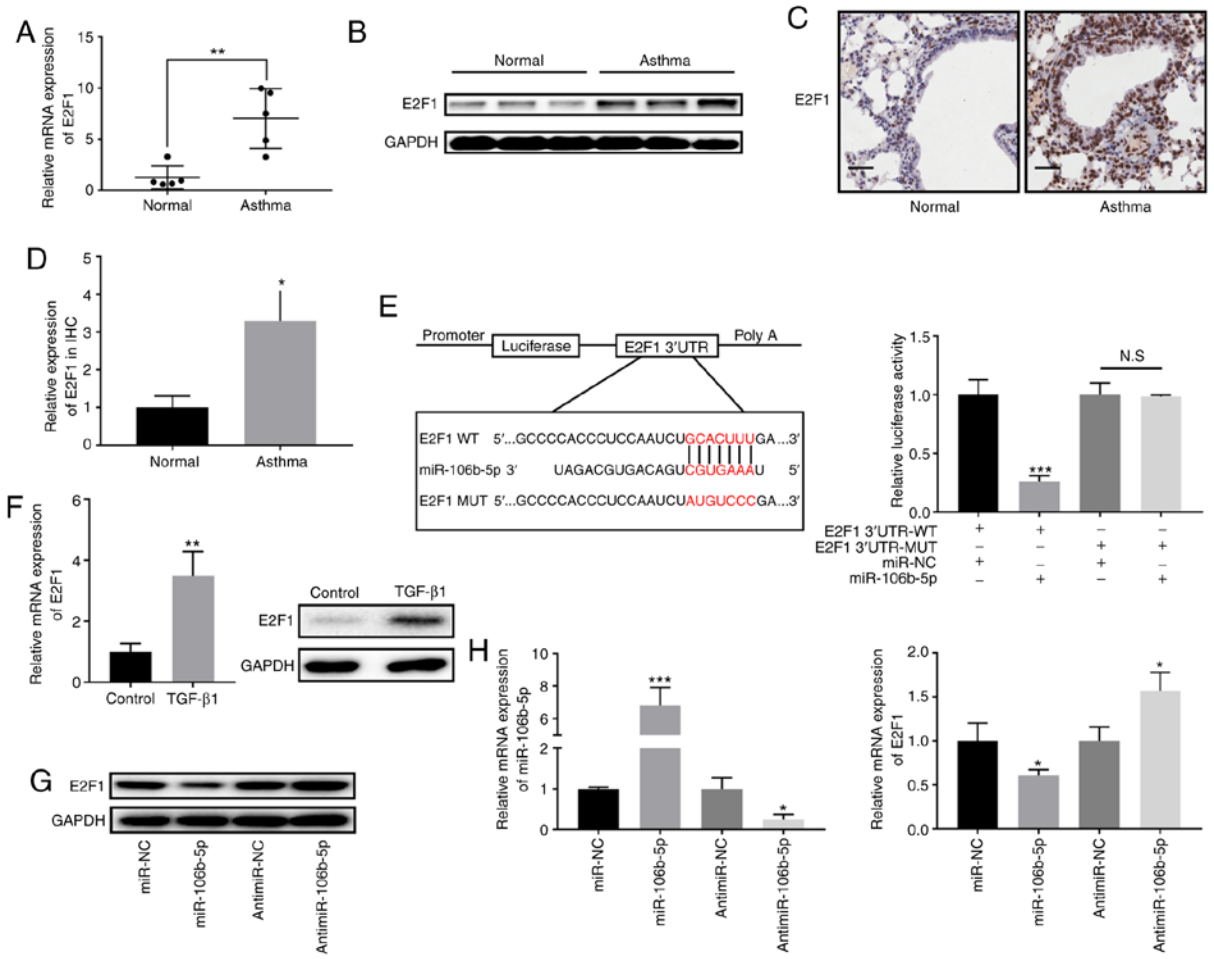

Figure 4. Association between miR-106b-5p and E2F1. (A) Relative E2F1 expression in asthmatic (n=5) and normal mice (n=5) was measured by RT-qPCR. (B) E2F1 protein expression in asthmatic and normal mice. (C) E2F1 expression in the lung tissues of asthmatic and normal mice was evaluated via IHC (scale bar, 50 μm). (D) Quantification of E2F1 expression according to IHC. (E) Schematic illustration of the miR-106b-5p binding site in E2F1 and the site mutagenesis (left panel). Luciferase reporter plasmids containing WT or MUT E2F1-3'-UTR were co-transfected into BEAS-2B cells with miR-106b-5p or miR-NC (right panel). (F) RT-qPCR and western blotting was performed to detect the mRNA and protein expression levels, respectively, of E2F1 in BEAS-2B cells after treatment with or without TGF-β1 (10 ng/ml) for 24 h. (G) E2F1 protein expression and (H) miR-106b-5p and E2F1 mRNA expression in miR-106b-5p-mimic- or antimiR-106b-5p-transfected BEAS-2B cells. Data are presented as the mean ± SD of three independent experiments. *P<0.05, **P<0.01 and ***P<0.001 vs. respective NCs. RT-qPCR, reverse transcription-quantitative PCR; NS, not significant; miR, microRNA; E2F1, E2F transcription factor 1; NC, negative control; UTR, untranslated region; WT, wild-type; MUT, mutant; IHC, immunohistochemistry.

activity. To further explore the association between E2F1 and SIX1, E2F1 was overexpressed or inhibited in BEAS-2B cells by siE2F1 or pE2F1 transfection (Fig. 5D and E). The results indicated that the mRNA and protein expression levels of SIX1 were decreased with siE2F1 and increased with pE2F1, compared with their respective negative controls (Fig. 5D and E). Additionally, the CHIP assay performed in BEAS-2B cells further suggested that E2F1 could bind to the promoter region of SIX1 *in vitro* (Fig. 5F).

E2F1- and SIX1-knockdown inhibits TGF-β1-induced fibrosis and EMT in BEAS-2B cells. To further clarify the role of E2F1, E2F1 expression was inhibited in BEAS-2B cells by siE2F1 transfection (Fig. 6A). siE2F1 decreased the TGF-β1-stimulated expression levels of fibronectin, α-SMA and collagen IV in BEAS-2B cells, indicating that E2F1-knockdown inhibited TGF-β1-stimulated fibrosis (Fig. 6B and D). Furthermore, siE2F1 ameliorated TGF-β1-stimulated increases in the expression levels of vimentin and N-cadherin, and TGF-β1-stimulated decreases in E-cadherin expression (Fig. 6C and E). The present results indicated that E2F1 silencing exhibited a similar phenotype to overexpressed miR-106b-5p in BEAS-2B cells. Additionally, siSIX1 was transfected in BEAS-2B cells to explore the function of SIX1 on fibrosis and EMT in asthma. RT-qPCR and western blotting were employed to measure SIX1 expression in siSIX1-transfected cells compared with in siNC-transfected cells (Fig. 6F). Western blot analysis revealed that inhibition of SIX1 reversed TGF-β1-induced upregulation of fibronectin, α-SMA, collagen IV, N-cadherin and vimentin proteins, and TGF-β1-induced downregulation of E-cadherin protein in BEAS-2B cells (Fig. 6G and H). The current results demonstrated that SIX1-knockdown impeded fibrosis and EMT in TGF-β1-induced BEAS-2B cells.

miR-106b-5p negatively regulates SIX1 via E2F1. To detect whether miR-106b-5p could negatively regulate SIX1 via E2F1, miR-106b-5p mimic and antimiR-106b-5p were co-transfected with pGL3-451 or pGL3-451 with mutation of E2F1 binding sites. The luciferase assay revealed that miR-106b-5p overexpression

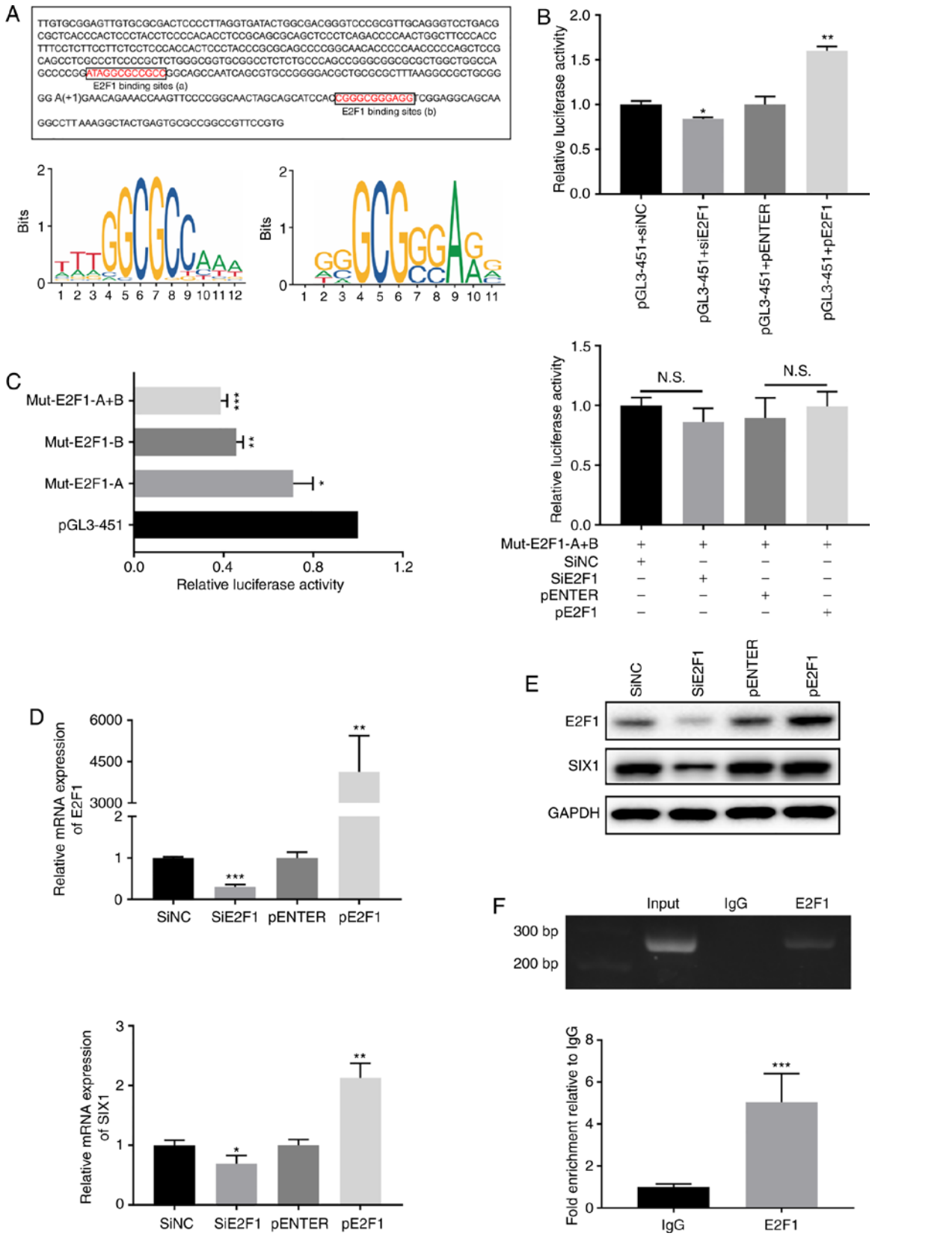

Figure 5. E2F1 positively regulates SIX1 at the transcription level. (A) Schematic representation of the putative binding sites for DNA-binding proteins in the promoter of the SIX1 gene. The putative transcription factor binding sites of E2F1 were outlined using black boxes (upper panel). Conserved base sequence of E2F1 binding site. The base size represents the binding affinity coefficient of transcription factor and promoter (lower panels). (B) Effect of E2F1 on promoter activity of SIX1. The luciferase activity in BEAS-2B cells co-transfected with pGL3-451 and plasmids containing siE2F1 or pE2F1. (C) Mutation analysis of the SIX1 promoter. Constructs fused to the firefly luciferase reporter vector were co-transfected into BEAS-2B cells with the *Renilla* luciferase expression vector. The level of firefly luciferase activity was normalized to *Renilla* luciferase activity (left panel). BEAS-2B cells were co-transfected with E2F1 overexpression plasmid or siE2F1 and mut-E2F1-A+B, respectively (right panel). (D) Relative E2F1 mRNA expression and (E) E2F1 and SIX1 protein expression in siE2F1- or pE2F1-transfected BEAS-2B cells. (F) Relative enrichment of E2F1 on the promoter region of SIX1 was detected by chromatin immunoprecipitation assay. Data are presented as the mean ± SD of three independent experiments. *P<0.05, **P<0.01 and ***P<0.001 vs. respective NCs. NS, not significant; miR, microRNA; E2F1, E2F transcription factor 1; SIX1, sine oculis homeobox homolog 1; NC, negative control; si, small interfering; mut, mutant.

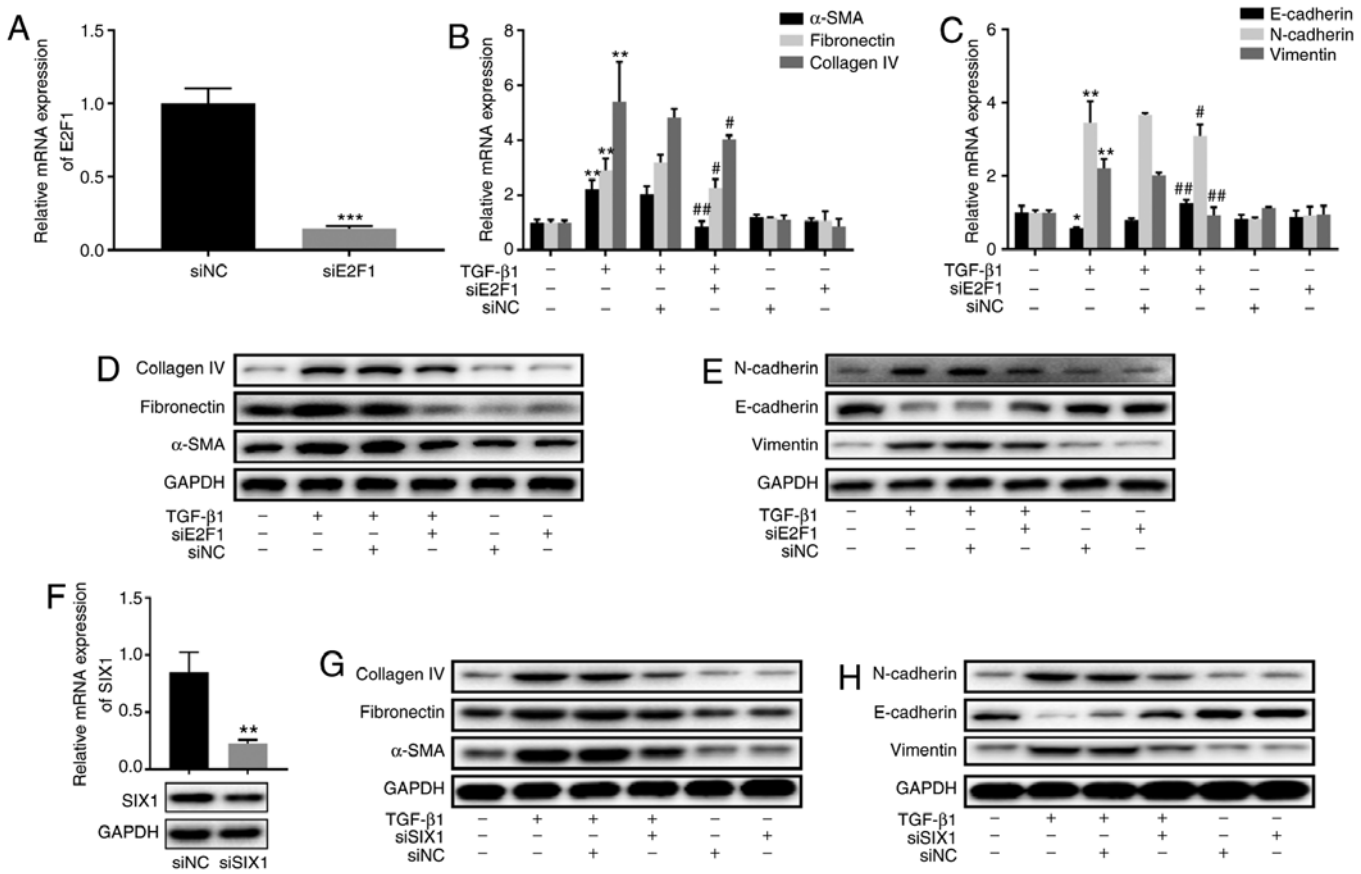

Figure 6. Effect of E2F1 and SIX1 on TGF-β1-induced fibrosis and EMT in BEAS-2B cells. (A) E2F1 expression following siNC or siE2F1 transfection in BEAS-2B cells was determined by RT-qPCR. (B) RT-qPCR was performed to assess the expression levels of fibrosis-associated proteins α-SMA, fibronectin and collagen IV in siE2F1-transfected BEAS-2B cells after treatment with or without TGF-β1 for 24 h. (C) RT-qPCR was employed to detect the mRNA expression levels of EMT-associated proteins E-cadherin, N-cadherin and vimentin in siE2F1-transfected BEAS-2B cells after treatment with or without TGF-β1 for 24 h. (D) Protein expression levels of fibrosis-associated proteins α-SMA, fibronectin and collagen IV in siE2F1-transfected BEAS-2B cells after treatment with or without TGF-β1 for 24 h. (E) Protein expression levels of EMT-associated proteins E-cadherin, N-cadherin and vimentin in siE2F1-transfected BEAS-2B cells after treatment with or without TGF-β1 for 24 h. (F) SIX1 expression in BEAS-2B cells was determined by RT-qPCR and western blotting. (G) Protein expression levels of fibrosis-associated proteins α-SMA, fibronectin and collagen IV in siSIX1-transfected BEAS-2B cells after treatment with or without TGF-β1 for 24 h. (H) Protein expression levels of EMT-associated proteins E-cadherin, N-cadherin and vimentin in siSIX1-transfected BEAS-2B cells after treatment with or without TGF-β1 for 24 h. Data are presented as the mean ± SD of three independent experiments. *P<0.05, **P<0.01 and ***P<0.001 vs. control. $^{\#}$P<0.05 and $^{\#\#}$P<0.01 vs. siNC+TGF-β1. miR, microRNA; E2F1, E2F transcription factor 1; SIX1, sine oculis homeobox homolog 1; NC, negative control; si, small interfering; RT-qPCR, reverse transcription-quantitative PCR; EMT, epithelial-mesenchymal transition; SMA, smooth muscle actin.

significantly inhibited luciferase activity in pGL3-451, but not in pGL3-451 with mutation of E2F1 binding sites (Fig. 7A). Meanwhile, miR-106b-5p-knockdown significantly promoted luciferase activity in pGL3-451, but not in pGL3-451 with mutation of E2F1 binding sites (Fig. 7A). Additionally, western blotting revealed that the miR-106b-5p-mediated decrease in SIX1 expression was partially rescued by co-transfection with pE2F1 (Fig. 7B). Subsequently, E2F1 binding to SIX1 promoter was examined in miR-106b-5p-mimic- and antimiR-106b-5p-transfected BEAS-2B cells. The level of E2F1 binding to SIX1 promoter was decreased in miR-106b-5p-mimic-transfected BEAS-2B cells, but increased after antimiR-106b-5p transfection (Fig. 7C). Overall, the present results suggested that miR-106b-5p could negatively regulate SIX1 expression in BEAS-2B cells via E2F1.

Discussion

Airway remodeling, an inevitable outcome of severe bronchial asthma (24), remains irreversible in severe asthma, despite advances in asthma treatment (25). Airway remodeling is caused by persistent damage to the airway epithelium and is manifested by subepithelial fibrosis, smooth muscle cell proliferation, mucus cell metaplasia and excessive deposition of extracellular matrix (ECM) (26). It has been previously demonstrated that airway remodeling can impair lung function of patients with asthma (27).

EMT has been demonstrated to contribute to airway remodeling, causing chronic inflammatory airway diseases such as asthma and chronic obstructive pulmonary disorder (28-30). During EMT, epithelial cells gradually lose their epithelial features and acquire mesenchymal characteristics, leading to airway remodeling and inflammation in asthma (31). Additionally, in patients with severe asthma, EMT decreases the sensitivity of airway epithelial cells to drug treatment and glucocorticoid therapy (32). In EMT, epithelial cell-cell adhesions are disrupted and mesenchymal membrane-associated proteins, such as N-cadherin and α-SMA, are upregulated, whereas epithelial adhesion molecules such as E-cadherin exhibit the opposite changes (11). Cell migration, alteration

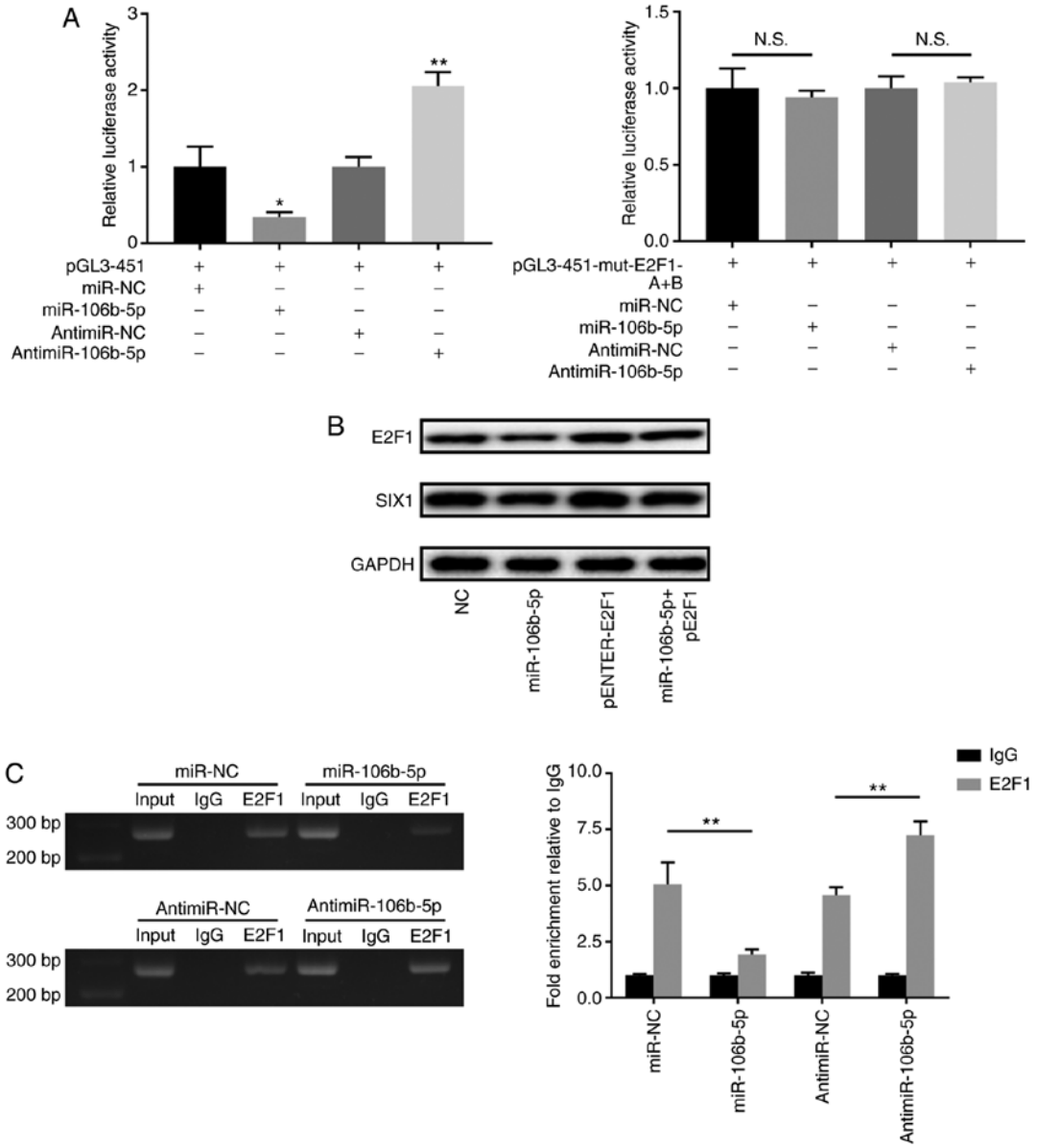

Figure 7. miR-106b-5p negatively regulates SIX1 via E2F1. (A) Relative luciferase activity in BEAS-2B cells co-transfected with pGL3-451 with miR-106b-5p or antimiR-106b-5p (left panel). Relative luciferase activity in BEAS-2B cells co-transfected with pGL3-451-mut-E2F1-A+B with miR-106b-5p or antimiR-106b-5p (right panel). (B) Protein expression levels of E2F1 and SIX1 in BEAS-2B cells after co-transfection with miR106b-5p and pE2F1 were detected by western blotting. (C) Relative enrichment of E2F1 containing miR-106b-5p- or antimiR-106b-5p-transfected on the promoter region of SIX1 was detected via chromatin immunoprecipitation assay. Data are presented as the mean ± SD of three independent experiments. *P<0.05 and **P<0.01 vs. respective NCs. NS, not significant; miR, microRNA; E2F1, E2F transcription factor 1; SIX1, sine oculis homeobox homolog 1; NC, negative control; si, small interfering; mut, mutant.

of ECM deposition and differentiation are other important molecular mechanisms involved in EMT (33). EMT may be caused by signaling molecules such as TGF-β1, bone morphogenetic proteins, epidermal growth factor, hepatocyte growth factor and fibroblast growth factor (33). TGF-β1 is a growth factor secreted by airway epithelial cells and infiltrating immune cells (34). Studies have revealed that patients with asthma have higher levels of TGF-β1 in bronchoalveolar lavage fluid and bronchial biopsy compared with the normal control group (35,36). A high level of TGF-β1 helps epithelial cells to transform fibroblasts into myofibroblasts, which contributes to the development of EMT (28,37,38).

miR-106b-5p serves a vital role in cancer progression, such as in glioma tumorigenesis (13), lung cancer (14), chronic myeloid leukemia (15), breast cancer (16,17) and hepatocellular carcinoma (18). However, to the best of our knowledge, there is no evidence on the function of miR-106b-5p in fibrosis and EMT in asthma. In the present study, miR-106b-5p expression was downregulated in asthmatic mice and TGF-β1-induced BEAS-2B cells, which highlighted that miR-106b-5p may inhibit TGF-β1-stimulated fibrosis in BEAS-2B cells. Subsequently, miR-106b-5p was found to inhibit the mesenchymal markers vimentin and N-cadherin, and promote the epithelial marker E-cadherin in TGF-β1-induced BEAS-2B cells. The opposite results were found after inhibiting miR-106b-5p. The present results suggested that E2F1, as a direct target for miR-106b-5p, may increase SIX1 expression by binding to its promoter region. Additionally, SIX1 was demonstrated to be a TGF-β1-inducible gene. To the best of our knowledge, the present study was the first to identify

the involvement of the miR-106b-5p/E2F1/SIX1 signaling pathway in asthma. Therefore, miR-106b-5p may be a potential therapeutic target for asthma.

Furthermore, the current data suggested that miR-106b-5p directly targeted the 3'-UTR of the E2F1 mRNA. Although E2F1 has been demonstrated to promote pathological liver fibrosis (39), its role in asthma has not been evaluated. Hence, the exact function of E2F1 in asthma was explored in the present study. It was revealed that the expression levels of the EMT-associated markers vimentin and N-cadherin were downregulated, while E-cadherin expression was upregulated in TGF-β1-induced BEAS-2B cells transfected with siE2F1. Additionally, the current data revealed that E2F1-knockdown effectively prevented TGF-β1-induced fibrosis *in vitro*, which was then reversed by co-transfection with the antimiR-106b-5p, indicating the critical role of E2F1 in preventing airway remodeling in asthma.

The present study further revealed that E2F1, a classical transcription factor, positively regulated SIX1 at the transcriptional level. Western blotting and RT-qPCR results demonstrated that E2F1 acted as a transcriptional inducer to enhance SIX1 expression. CHIP and luciferase assays further confirmed this hypothesis.

In conclusion, the present study identified that miR-106b-5p inhibited fibrosis and EMT via the miR-106b-5p/E2F1/SIX1 signaling pathway in TGF-β1-induced BEAS-2B cells. Therefore, miR-106b-5p may be a potential therapeutic target for asthma.

Acknowledgements

Not applicable.

Funding

The present study was supported by the National Natural Science Foundation of China (grant nos. 81970579 and 81972954).

Availability of data and materials

All data generated or analyzed during this study are included in this published article.

Authors' contributions

SL mainly designed the experiments and wrote the manuscript. XC and XW contributed to performing the cell experiments and reviewing the manuscript. SZ, XD and JC designed and conducted the animal experiments. SL, XC, XW, SZ, XD and JC contributed to data analysis. GZ mainly constructed the idea of this article and provided administrative, technical and material support. SL, XC and GZ were responsible for confirming the authenticity of the data. All authors read and approved the final manuscript.

Ethics approval and consent to participate

The study was approved by the Nanjing Medical University Animal Experimental Ethics Committee (approval no. 2005020).

Patient consent for publication

Not applicable.

Competing interests

The authors declare that they have no competing interests.

References

1. Ellwood P, Asher MI, Billo NE, Bissell K, Chiang CY, Ellwood EM, El-Sony A, García-Marcos L, Mallol J, Marks GB, *et al*: The Global Asthma Network rationale and methods for Phase I global surveillance: Prevalence, severity, management and risk factors. Eur Respir J 49: 1601605, 2017.
2. Prasad B, Nyenhuis SM, Imayama I, Siddiqi A and Teodorescu M: Asthma and obstructive sleep apnea overlap: What has the evidence taught Us? Am J Respir Crit Care Med 201: 1345-1357, 2020.
3. Woodcock A, Vestbo J, Bakerly ND, New J, Gibson JM, McCorkindale S, Jones R, Collier S, Lay-Flurrie J, Frith L, *et al*: Effectiveness of fluticasone furoate plus vilanterol on asthma control in clinical practice: An open-label, parallel group, randomised controlled trial. Lancet 390: 2247-2255, 2017.
4. Sharma P, Yi R, Nayak AP, Wang N, Tang F, Knight MJ, Pan S, Oliver B and Deshpande DA: Bitter taste receptor agonists mitigate features of allergic asthma in mice. Sci Rep 7: 46166, 2017.
5. Breton JD, Heydet D, Starrs LM, Veldre T and Ghildyal R: Molecular changes during TGFβ-mediated lung fibroblast-myofibroblast differentiation: Implication for glucocorticoid resistance. Physiol Rep 6: e13669, 2018.
6. Aquino-Jarquin G: Emerging role of CRISPR/Cas9 technology for MicroRNAs editing in cancer research. Cancer Res 77: 6812-6817, 2017.
7. Giroux P, Bhajun R, Segard S, Picquenot C, Charavay C, Desquilles L, Pinna G, Ginestier C, Denis J, Cherradi N and Guyon L: miRViz: A novel webserver application to visualize and interpret microRNA datasets. Nucleic Acids Res 48: W252-W261, 2020.
8. Yu L, Xu J, Liu J, Zhang H, Sun C, Wang Q, Shi C, Zhou X, Hua D, Luo W, *et al*: The novel chromatin architectural regulator SND1 promotes glioma proliferation and invasion and predicts the prognosis of patients. Neuro Oncol 21: 742-754, 2019.
9. Lu G, Li Y, Ma Y, Lu J, Chen Y, Jiang Q, Qin Q, Zhao L, Huang Q, Luo Z, *et al*: Long noncoding RNA LINC00511 contributes to breast cancer tumourigenesis and stemness by inducing the miR-185-3p/E2F1/Nanog axis. J Exp Clin Cancer Res 37: 289, 2018.
10. Wang CJ, Zhu CC, Xu J, Wang M, Zhao WY, Liu Q, Zhao G and Zhang ZZ: Correction to: The lncRNA UCA1 promotes proliferation, migration, immune escape and inhibits apoptosis in gastric cancer by sponging anti-tumor miRNAs. Mol Cancer 18: 129, 2019.
11. Du X, Tu Y, Liu S, Zhao P, Bao Z, Li C, Li J, Pan M and Ji J: LINC00511 contributes to glioblastoma tumorigenesis and epithelial-mesenchymal transition via LINC00511/miR-524-5p/YB1/ZEB1 positive feedback loop. J Cell Mol Med 24: 1474-1487, 2020.
12. Chiba Y and Misawa M: MicroRNAs and their therapeutic potential for human diseases: MiR-133a and bronchial smooth muscle hyperresponsiveness in asthma. J Pharmacol Sci 114: 264-268, 2010.
13. Liu F, Gong J, Huang W, Wang Z, Wang M, Yang J, Wu C, Wu Z and Han B: MicroRNA-106b-5p boosts glioma tumorigensis by targeting multiple tumor suppressor genes. Oncogene 33: 4813-4822, 2014.
14. Chen Z, Chen X, Lei T, Gu Y, Gu J, Huang J, Lu B, Yuan L, Sun M and Wang Z: Integrative analysis of NSCLC identifies LINC01234 as an oncogenic lncRNA that interacts with HNRNPA2B1 and regulates miR-106b biogenesis. Mol Ther 28: 1479-1493, 2020.
15. Yang J, Yin Z, Li Y, Liu Y, Huang G, Gu C and Fei J: The identification of long non-coding RNA H19 target and its function in chronic myeloid leukemia. Mol Ther Nucleic Acids 19: 1368-1378, 2020.
16. Wang Z, Li TE, Chen M, Pan JJ and Shen KW: miR-106b-5p contributes to the lung metastasis of breast cancer via targeting CNN1 and regulating Rho/ROCK1 pathway. Aging (Albany NY) 12: 1867-1887, 2020.

17. Lee J, Kim HE, Song YS, Cho EY and Lee A: miR-106b-5p and miR-17-5p could predict recurrence and progression in breast ductal carcinoma in situ based on the transforming growth factor-beta pathway. Breast Cancer Res Treat 176: 119-130, 2019.
18. Gu H, Gu S, Zhang X, Zhang S, Zhang D, Lin J, Hasengbayi S and Han W: miR-106b-5p promotes aggressive progression of hepatocellular carcinoma via targeting RUNX3. Cancer Med 8: 6756-6767, 2019.
19. Fornes O, Castro-Mondragon JA, Khan A, van der Lee R, Zhang X, Richmond PA, Modi BP, Correard S, Gheorghe M, Baranašić D, *et al*: JASPAR 2020: Update of the open-access database of transcription factor binding profiles. Nucleic Acids Res 48: D87-D92, 2020.
20. Feng DD, Cao Q, Zhang DQ, Wu XL, Yang CX, Chen YF, Yu T, Qi HX and Zhou GP: Transcription factor E2F1 positively regulates interferon regulatory factor 5 expression in non-small cell lung cancer. OncoTargets Ther 12: 6907-6915, 2019.
21. Livak KJ and Schmittgen TD: Analysis of relative gene expression data using real-time quantitative PCR and the 2(-Delta Delta C(T)) method. Methods 25: 402-408, 2001.
22. Young K and Morrison H: Quantifying microglia morphology from photomicrographs of immunohistochemistry prepared tissue using imagej. J Vis Exp: 57648, 2018.
23. Yang ZC, Yi MJ, Shan YC, Wang C, Ran N, Jin LY, Fu P, Feng XY, Xu L and Qu ZH: Targeted inhibition of Six1 attenuates allergic airway inflammation and remodeling in asthmatic mice. Biomed Pharmacother 84: 1820-1825, 2016.
24. Olafsdottir TA, Theodors F, Bjarnadottir K, Bjornsdottir US, Agustsdottir AB, Stefansson OA, Ivarsdottir EV, Sigurdsson JK, Benonisdottir S, Eyjolfsson GI, *et al*: Eighty-eight variants highlight the role of T cell regulation and airway remodeling in asthma pathogenesis. Nat Commun 11: 393, 2020.
25. Bertolini F, Carriero V, Bullone M, Sprio AE, Defilippi I, Sorbello V, Gani F, Di Stefano A and Luigi Massimo Ricciardolo F: Correlation of matrix-related airway remodeling and bradykinin B1 receptor expression with fixed airflow obstruction in severe asthma. Allergy: Dec 7, 2020 (Epub ahead of print).
26. Vignola AM, Kips J and Bousquet J: Tissue remodeling as a feature of persistent asthma. J Allergy Clin Immunol 105: 1041-1053, 2000.
27. Ward C, Pais M, Bish R, Reid D, Feltis B, Johns D and Walters EH: Airway inflammation, basement membrane thickening and bronchial hyperresponsiveness in asthma. Thorax 57: 309-316, 2002.
28. Hackett TL, Warner SM, Stefanowicz D, Shaheen F, Pechkovsky DV, Murray LA, Argentieri R, Kicic A, Stick SM, Bai TR and Knight DA: Induction of epithelial-mesenchymal transition in primary airway epithelial cells from patients with asthma by transforming growth factor-beta1. Am J Respir Crit Care Med 180: 122-133, 2009.
29. Wang Y, Jia M, Yan X, Cao L, Barnes PJ, Adcock IM, Huang M and Yao X: Increased neutrophil gelatinase-associated lipocalin (NGAL) promotes airway remodelling in chronic obstructive pulmonary disease. Clin Sci (Lond) 131: 1147-1159, 2017.
30. Gorowiec MR, Borthwick LA, Parker SM, Kirby JA, Saretzki GC and Fisher AJ: Free radical generation induces epithelial-to-mesenchymal transition in lung epithelium via a TGF-β1-dependent mechanism. Free Radic Biol Med 52: 1024-1032, 2012.
31. Hackett TL: Epithelial-mesenchymal transition in the pathophysiology of airway remodelling in asthma. Curr Opin Allergy Clin Immunol 12: 53-59, 2012.
32. Ijaz T, Pazdrak K, Kalita M, Konig R, Choudhary S, Tian B, Boldogh I and Brasier AR: Systems biology approaches to understanding epithelial mesenchymal transition (EMT) in mucosal remodeling and signaling in asthma. World Allergy Organ J 7: 13, 2014.
33. Thiery JP and Sleeman JP: Complex networks orchestrate epithelial-mesenchymal transitions. Nat Rev Mol Cell Biol 7: 131-142, 2006.
34. Ito J, Harada N, Nagashima O, Makino F, Usui Y, Yagita H, Okumura K, Dorscheid DR, Atsuta R, Akiba H and Takahashi K: Wound-induced TGF-β1 and TGF-β2 enhance airway epithelial repair via HB-EGF and TGF-α. Biochem Biophys Res Commun 412: 109-114, 2011.
35. Chakir J, Shannon J, Molet S, Fukakusa M, Elias J, Laviolette M, Boulet LP and Hamid Q: Airway remodeling-associated mediators in moderate to severe asthma: Effect of steroids on TGF-beta, IL-11, IL-17, and type I and type III collagen expression. J Allergy Clin Immunol 111: 1293-1298, 2003.
36. Yamaguchi M, Niimi A, Matsumoto H, Ueda T, Takemura M, Matsuoka H, Jinnai M, Otsuka K, Oguma T, Takeda T, *et al*: Sputum levels of transforming growth factor-beta1 in asthma: Relation to clinical and computed tomography findings. J Investig Allergol Clin Immunol 18: 202-206, 2008.
37. Warburton D, Schwarz M, Tefft D, Flores-Delgado G, Anderson KD and Cardoso WV: The molecular basis of lung morphogenesis. Mech Dev 92: 55-81, 2000.
38. Holgate ST, Davies DE, Puddicombe S, Richter A, Lackie P, Lordan J and Howarth P: Mechanisms of airway epithelial damage: Epithelial-mesenchymal interactions in the pathogenesis of asthma. Eur Respir J Suppl 44: 24s-29s, 2003.
39. Zhang Y, Xu N, Xu J, Kong B, Copple B, Guo GL and Wang L: E2F1 is a novel fibrogenic gene that regulates cholestatic liver fibrosis through the Egr-1/SHP/EID1 network. Hepatology 60: 919-930, 2014.